Diffuse soil CO_2 degassing from Linosa island

Dario Cellura[1], Vincenzo Stagno[2], Marco Camarda[3,*], Mariano Valenza[1]

[1] *Università degli Studi di Palermo, Dipartimento di Scienze della Terra e del Mare (DSTM), Palermo, Italy*

[2] *Carnegie Institution of Washington, Geophysical Laboratory, Washington, DC, USA*

[3] *Istituto Nazionale di Geofisica e Vulcanologia, Sezione di Palermo, Palermo, Italy*

Article history
Received December 12, 2013; accepted May 21, 2014.
Subject classification:
Fluid geochemistry, CO_2, Soil degassing, Volcano monitoring, Instruments and techniques.

ABSTRACT

Herein, we present and discuss the result of 148 measurements of soil CO_2 flux performed for the first time in Linosa island (Sicily Channel, Italy), a Plio-Pleistocene volcanic complex no longer active but still of interest owing to its location within a seismically active portion of the Sicily Channel rift system. The main purpose of this survey was to assess the occurrence of CO_2 soil degassing, and compare flux estimations from this island with data of soil degassing from worldwide active volcanic as well as non-volcanic areas. To this aim soil CO_2 fluxes were measured over a surface of about 4.2 km^2 covering ~80% of the island. The soil CO_2 degassing was observed to be mainly concentrated in the eastern part of the island likely due to volcano-tectonic lineaments, the presence of which is in good agreement with the known predominant regional faults system. Then, the collected data were interpreted using sequential Gaussian simulation that allowed estimating the total CO_2 emissions of the island. Results show low levels of CO_2 emissions from the soil of the island (~55 ton d^{-1}) compared with CO_2 emissions of currently active volcanic areas, such as Miyakejima (Japan) and Vulcano (Italy). Results from this study suggest that soil degassing in Linosa is mainly fed by superficial organic activity with a moderate contribution of a deep CO_2 likely driven by NW-SE trending active tectonic structures in the eastern part of the island.

1. Introduction

The release of gases such as CO_2 from the soil is a common process that occurs in both tectonic and volcano-tectonic areas. In active volcanic areas, large amounts of CO_2 are released from ascending magmas or generated by crystallization of deep magma bodies [Harris and Rose 1996, Camarda et al. 2012]. Part of this CO_2 is released into the atmosphere through summit craters, while another part is emitted from the soil along the flanks of volcanoes. In non-volcanic environments, moderate to strong emission of CO_2 are usually encountered in areas with the occurrence of active tectonic structures, such as faults and fractures, which constitutes highly permeable preferential pathways for natural emissions of deep gases. Because tectonic lineaments are often buried by soil and/or sediments that act as a gas diffuser, measurements of gas emissions from soil can provide useful information regarding the presence of hidden and/or active faults [Giammanco et al. 1997, Ciotoli et al. 1998, Lewicki and Brantley 2000, Guerra and Lombardi 2001, De Gregorio et al. 2002, Aiuppa et al. 2004, Giammanco et al. 2006], as well as changes in the in feeding system of active volcanic areas [Giammanco et al. 1995, Federico et al. 2011, Camarda et al. 2012].

Here we discuss the results of a soil CO_2 flux survey performed in Linosa island. The island is located in the south-western part of the Mediterranean Sea (see Figure 1), and with Pantelleria island constitutes part of the Sicily Channel rift system (SCrs). Volcanism occurred at Linosa island in the late Plio-Pleistocene [Lodolo et al. 2012, and references therein], while there is no evidence of current volcanic activity, such as fumaroles or thermal waters. Only few submarine exhalative manifestations were identified near the top of a submerged relict volcanic structure located in the SW offshore of the island [Lanti et al. 1988].

The main aim of this study was to investigate the soil CO_2 flux in a volcanic island with no signs of a recent volcanic activity but located in a currently active seismic area. The results of this study can contribute to extend our knowledge of the global CO_2 emissions within volcanic and non-volcanic areas [Burton et al. 2013].

2. Regional and local tectonic setting

The Sicily Channel rift system (Figure 1) formed as consequence of the continental rifting process that affected the northern margin of the African plate since the Late Miocene in response to the opening of the Tyrrhenian Sea [Boccaletti et al. 1987]. It is characterized by three main tectonic depressions known as Pan-

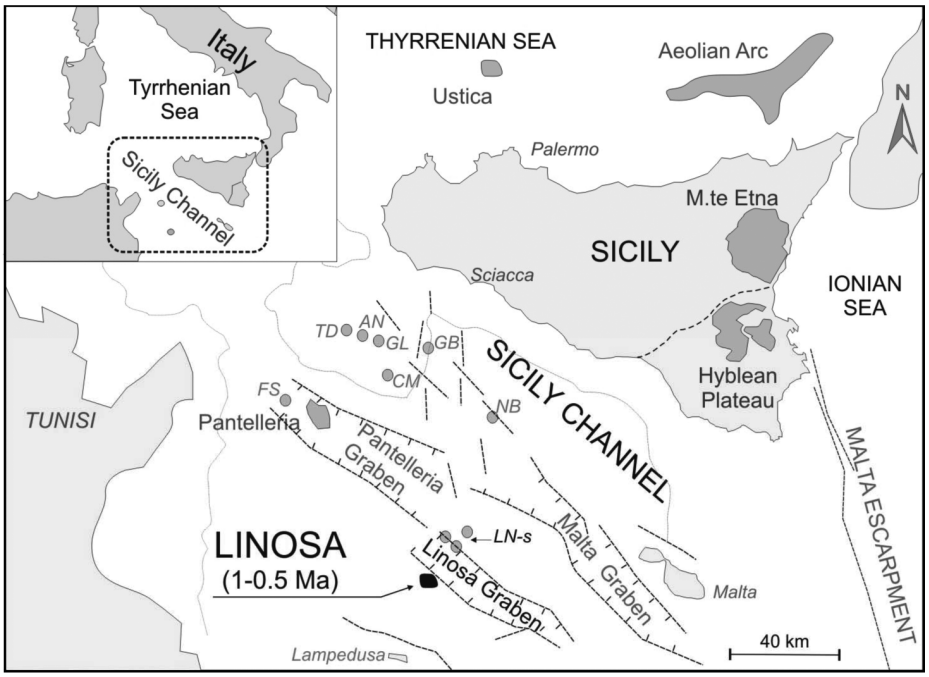

Figure 1. Geographic sketch of the Sicily Channel Rift with the location of Linosa island (fully black). The main regional volcanic manifestations are also reported (heavy grey); seamounts: AN = Anfitrite; CM = Cimotoe; FS = Foerstner; GB = Graham Bank; GL = Galatea; LN-S = Linosa-seamounts; NB = Nameless Bank; TD = Tetide.

telleria, Linosa and Malta grabens with depths of 1350, 1580 and 1720 m below sea level (b.s.l.), respectively [Grasso et al. 1991, Civile et al. 2010]. The uprising of the asthenosphere to 60 km in depth [Della Vedova et al. 1989], and the thinning of the African foreland continental crust [Scarascia et al. 2000] resulted in the formation of widespread volcanism that characterized the Sicily Channel. The formation of the short-lived island of Ferdinandea in 1831 from the Graham Bank area [Gemmellaro 1831] and the submarine eruption of the volcano Foerstner in 1891 [Washington 1909] sited 5 km NW of Pantelleria island, were described as the last two volcanic events responsible of a wide range of products from basalt to trachytic/pantelleritic composition with different geochemical affinity, such as tholeiitic, alkaline, and peralkaline [Rotolo et al. 2006]. Thermal and bubbling springs, mofettes and fumaroles are all present in Pantelleria island. In addition, the actual seismic activity [Schorlemmer et al. 2010] is recorded principally near the axial zone of the Sicily Channel (Linosa and Pantelleria Grabens).

Located about 160 km south of the southern Sicilian coast in the Pelagian Archipelago (Figure 1), Linosa island (about 5.2 km^2; 196 m a.s.l.) represents the subaerial portion of a larger volcanic complex rising from a depth of 800 m b.s.l. near the south-west sector of the homonymous graben [Calanchi et al. 1989]. The influence of the regional tectonic trends (NW-SE and NNW-SSE) on the volcanic evolution of the island can be inferred both by the distribution of the inland and offshore volcanic centers (i.e. the ancient submerged volcanic center of Secca di Tramontana and a shoal in the SE margin), and by the maximum axis of elongation of some principal edifices, such as Montagna Rossa and Pozzo Salito (Figure 2). These edifices represent the most ancient sub-aerial volcanic complexes in the SCrs dated 1.06 $\pm$ 0.10 and 0.53 $\pm$ 0.07 Ma [Lanzafame et al. 1994].

3. Soil CO_2 flux measurements and sampling method

3.1. Materials and methods

We performed 148 measurements of soil CO_2 flux during the summer in 2006. The measurement points were distributed over a surface of about 4.2 km^2 (80% of the entire area) passing through all the main eruptive centers of the island (Monte Vulcano, Montagna Rossa, Monte Nero, Timpone, Monte Bancarella, Fossa Cappellano and Pozzo Salito; see Figure 2), with the exception of some lava fields located along the NW and SW side of the island (Caletta and Arena Bianca). In these last areas the soil was found to be totally absent or not thick enough to perform CO_2 flux measurement with the method described hereinafter. The soil gas investigation was carried out with a mean distance of 150 m between adjacent measurement points, chosen as a good compromise between the detail of the survey and the extent of the investigated area. It is known that the diffuse degassing from soil is influenced by atmospheric conditions [Diliberto et al. 2002, Granieri et al. 2003, Rinaldi et al. 2012]. To minimize the effect of

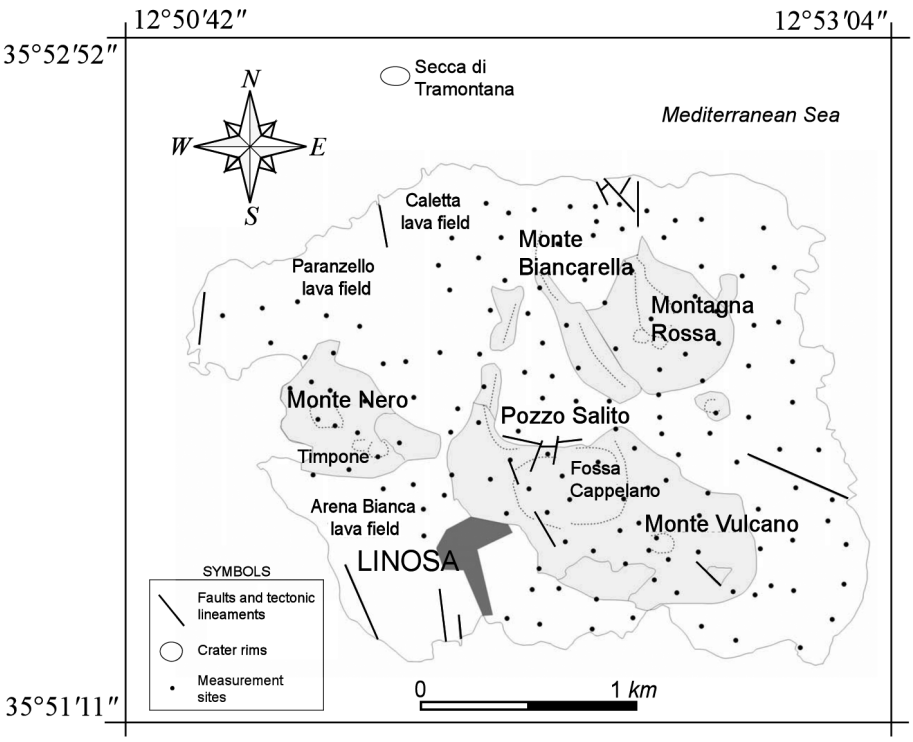

Figure 2. Simplified representation of the island of Linosa with the main tectonic lineaments (black lines) and volcanic centers (grey areas and dotted lines) (modified after Lanzafame et al. [1994]). Black points indicate the location of measurements for the soil CO_2 flux.

the variability of atmospheric conditions the measurements were conducted within few hours during the day, implying a negligible temperature variation.

Measurements of CO_2 diffuse degassing were performed using the dynamic concentration method [Gurrieri and Valenza 1988, Camarda et al. 2006b]. This method consists of measuring the CO_2 concentration in a mixture of air and soil gas that has been generated in a specifically designed probe inserted into the soil to a depth of ~50 cm. The gas mixture is then obtained by producing a very small negative pressure in the probe using a pump at a constant flux of 0.8 L min^{-1}. The mixture is subsequently analyzed using an infrared (IR) Gascard II spectrophotometer provided by Edinburgh Instruments Ltd. After a given time of pump activation (generally less than 1 minute), a constant CO_2 concentration is measured in the gas mixture, that is the dynamic concentration C_d [Camarda et al. 2006b]. The relationship used to convert dynamic concentration values to CO_2 flux was calibrated after laboratory measurements during which several measurements of C_d were collected in a soil layer fed by known and constant CO_2 fluxes [Camarda et al. 2006b]. Several tests were performed using soils with different values of gas permeability and porosity in order to evaluate the influence of soil permeability on the calculated CO_2 fluxes. These results revealed that the propagated error in the flux calculation is generally less than 5% for soils with gas permeability varying between 0.36 and 123 darcy [Camarda et al. 2006b].

Due to the absence of values of gas permeability for the soils of Linosa, we considered a value of soil gas permeability of 37 darcy used to calculate the CO_2 flux from all the 148 measurement points with dynamic method. This value corresponds to the average value of gas permeability estimated for the soils in Vulcano island, Sicily [Camarda et al. 2006a]. The soil gas permeability in this island ranges between 5 darcy (fine sand) and 80 darcy (coarse sand). Other values of gas permeability of volcanic soils were reported by Moldrup et al. [2003], where the air permeability of some volcanic ash soils were determined from three locations in Japan. In this case the reported values ranged from 1.8 to 168 darcy with a mean value of 31 darcy. Additional data available in literature generally refer to water permeability and cannot be used to accurately assess the value of gas permeability of volcanic soils due to the known Klinkenberg effect [Klinkenberg 1941]. Therefore, our value of 37 darcy can be considered representative for gas permeability of soils in Linosa island.

Further uncertainties in measurements of CO_2 from soil using the dynamic concentration method might be introduced by pressure variations during the field measurements. However, owing to the almost flat topography of the island (max altitude of ~190 meters), possible errors can be considered negligible (about ±3% of range).

During the survey three gaseous samples were collected in those sites with the highest CO_2 fluxes to determine their carbon isotopic composition. Gases were

sampled from the soil at a depth of 50 cm using a Teflon tube of 5 mm in diameter connected to a syringe, and then stored in glass flasks equipped with vacuum stopcocks. The carbon isotopic composition of CO_2 was determined using a Finnigan Mat Delta Plus Mass Spectrometer. Measured isotopic values are expressed as $\delta^{13}C(CO_2)$ *versus* the Pee Dee Belemnite (PDB) standard and characterized by uncertainties of ±0.2‰.

3.2. Sequential Gaussian simulation and estimation of total CO_2 flux

Sequential Gaussian Simulation (SGSIM) was performed with the aim to map the spatial variation of soil degassing and calculate the total CO_2 output of the island.

The (SGSIM) was performed using the Stanford Geostatistical Modeling Software (SGeMS), an open-source package developed by the Stanford Center for Reservoir Forecasting for solving problems involving spatially related variable [Remy 2005]. To perform SGSIM the distribution of data must be Gaussian. Therefore, as first step, all fluxes were normalized in order to obtain a distribution with mean and variance being equal to 0 and 1, respectively. Then, the semivariogram of normalized data was determined in order to examine the spatial variability of the measured soil CO_2 fluxes.

Further technical details of the SGSIM consisted of, (1) definition of the grid of the simulation; (2) definition of a random path visiting each node of the grid area; (3) random choice of the node in the sampled grid; (4) estimation at each node of the mean value and the variance of the local conditional cumulative distribution function (CCDF) by using simple kriging algorithm considering the semivariogram of the normalized data; (5) drawing of a value from that Gaussian CCDF and addition of the simulated value to the data set; (6) proceeding to the next node in the path and repeating the (4) and (5) steps until all nodes have been visited.

The total CO_2 output emitted from the soils of the island of Linosa and its relative uncertainty were obtained as the mean and the standard deviation of the total soil CO_2 flux estimated for each of the 100 simulations. These flux values were calculated for each simulation integrating over the grid area the average value of the soil CO_2 flux given by the SGSIM.

4. Results and discussion

4.1. Statistical analysis of the soil CO_2 fluxes

The data relative to the measured dynamic concentrations (C_d) and the calculated fluxes are shown in Table S1 along with the coordinates of each measurement point (see Supplementary files). The values of

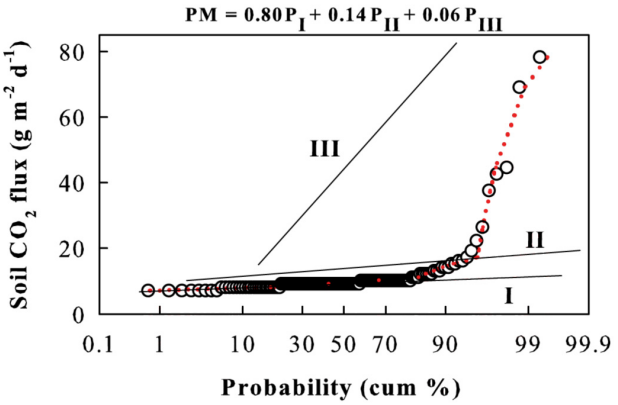

Figure 3. Probability plot of soil CO_2 fluxes measured on the island. The red dotted curve shows the theoretical distribution produced by combining the populations in the proportions indicated by the threshold values according to the equation reported at the top of the graph. Solid lines indicate the populations reconstructed according to the procedure illustrated by Sinclair [1974].

soil CO_2 flux collected during the survey showed a small variation between 12 and 78 g m^{-2} d^{-1}, with a mean value of 11 g m^{-2} d^{-1}. This range of fluxes is lower than that observed in active volcanic areas, such as the island of Vulcano and Mount Etna (Italy), where the measured soil CO_2 fluxes generally display values up to three orders of magnitude [Chiodini et al. 1998, Camarda et al. 2012]. The high variability of soil CO_2 fluxes observed in active volcanic areas can be manly explained as due to mixing between CO_2 with different origin such as (a) microbial decomposition of soil organic matter and root respiration, and (b) emissions from a deep degassing source [Camarda et al. 2007, Chiodini et al. 2008]. As a consequence, the resulting statistical distribution is expected to be, at least, bimodal.

In this study, although the observed low variability of soil CO_2 fluxes, we constructed a normal probability plot (PP) of the soil CO_2 fluxes at the aim to discriminate populations of data ascribable to different sources [Sinclair 1974, Chiodini et al. 2008]. This type of plot shows the cumulative frequencies (X axis) of the measured soil CO_2 fluxes (Y axis; Figure 3) on a probability scale. Data that are normally distributed will appear in this plot as a straight line. The presence of multiple straight lines with different slopes indicates, therefore, the presence of various populations of data with normal distribution but with diverse ori-

CO_2 flux populations	Mean CO_2 flux (g m^{-2} d^{-1})	Standard deviation	Proportion
I	9	1	80
II	13	2	14
III	43	21	6

Table 1. Summary statistics for the portioned CO_2 flux populations.

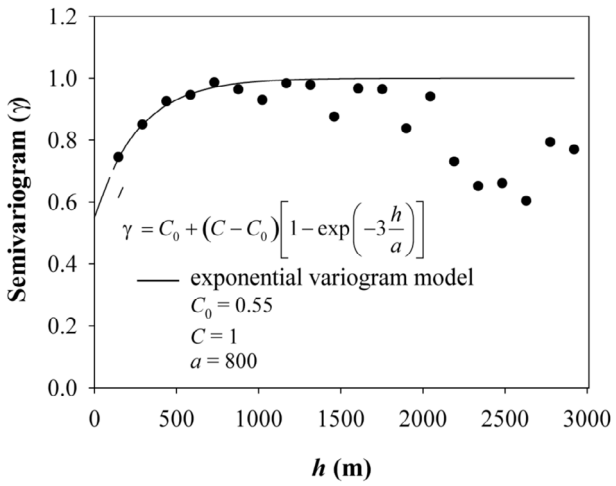

Figure 4. Variogram of normal scores of the soil CO_2 flux.

gin of the CO_2. The PP of all field measurements performed for this study displayed this feature. Figure 3 shows the PP of the soil CO_2 flux data measured in Linosa island during August 2006. The PP shows two inflection points reflecting three overlapping populations of data with normal distributions, a low-flux group (population I), an intermediate-flux group (population II), and a high-flux group (population III). The main statistics of these populations are listed in Table 1. To test the validity of the three-population model we also compared the theoretical distribution resulting from the combination of the portioned populations (dotted line in Figure 3) with the actual data distribution (empty circles in Figure 3). A good agreement between the real and ideal distributions was found, as proof of the high goodness of the three-population model. In particular, the population I is characterized by low fluxes with a mean value of 9 g m^{-2} d^{-1} and a standard deviation of 1 g m^{-2} d^{-1}. These low values are consistent with typical values reported for superficial soil respiration (3.6–13.7 g m^{-2} d^{-1}, Monteith et al. [1964]; 6–11 g m^{-2} d^{-1}, Brown and Rosenberg [1971]). The population III is characterized by a mean value of 43 g m^{-2} d^{-1} and standard deviation of 21 g m^{-2} d^{-1}, and can be considered as the anomalous population, likely suggesting the possible contribution of a deeper source of CO_2. The intermediate population II shows a mean value of 13 g m^{-2} d^{-1} with a standard deviation of 2 g m^{-2} d^{-1}. This flux group can be explained assuming mixing of shallower biogenic CO_2 and CO_2 of deep origin [Chiodini et al. 2008]. Alternatively, the population II can also be ascribed to the biogenic superficial activity, being its flux consistent with those values typically reported for soil respiration. In this case, we would have two different background populations (I and II) that, for instance, may be related to the presence of different types of vegetation in the island.

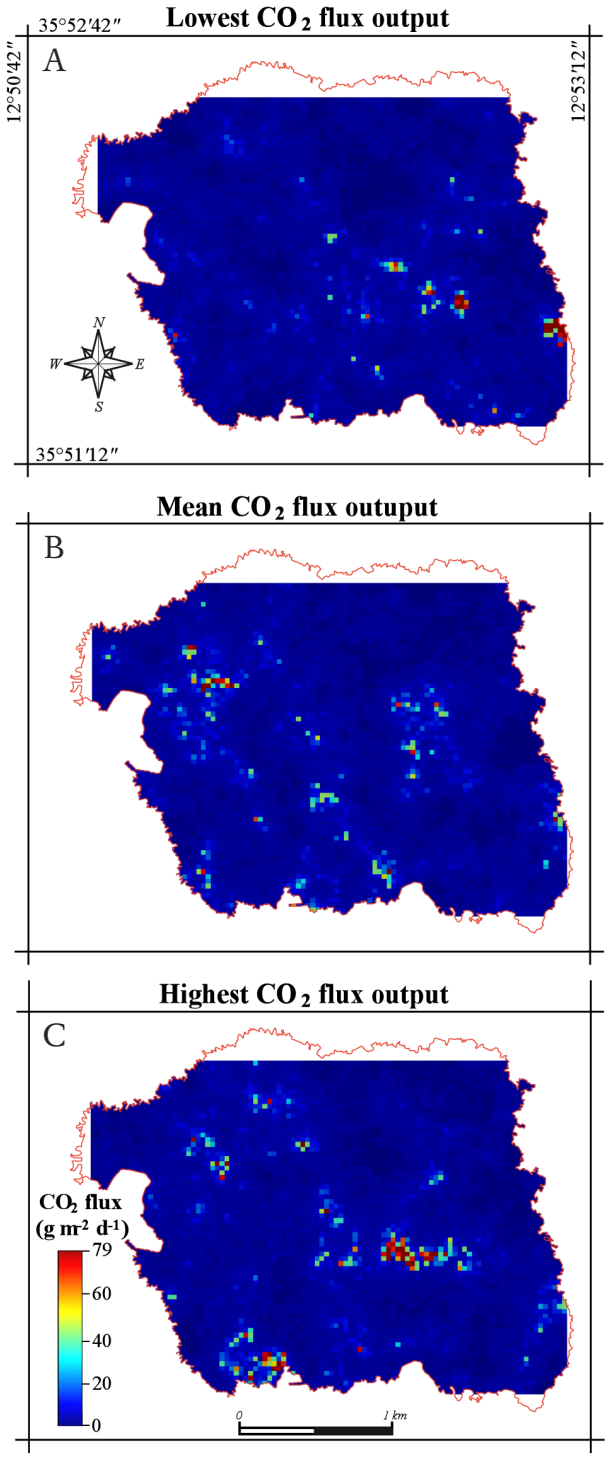

Figure 5. Maps of soil CO_2 flux. From the top to the bottom, the map relative to the realization giving the lowest value of the soil CO_2 flux output, the map relative to the realization giving the mean value of the soil CO_2 flux output, and the map relative to the realization giving the highest value of the soil CO_2 flux output.

4.2. Mapping soil CO_2 flux and total CO_2 output

The experimental semivariogram of the normalized data (Figure 4) has been computed and fitted by the following standardized exponential model,

$$\gamma = C_0 + (C - C_0)\left[1 - \exp\left[-3\frac{h}{a}\right]\right]$$

The values assumed by the nugget (C_0), the sill (C) and the range (a) are reported in Figure 4 and are here used in the SGeMS software to adjust the model of the SGSIM.

Figure 5 shows three examples of maps representative of low, intermediate and high flux, respectively (A, B and C). The spatial distribution of soil CO_2 flux is significantly different for the three cases. Areas with high flux resulting from one simulation may have lower flux resulting from another simulation. However, the different simulations are equiprobable and "honor" the experimental data in the sense described by Journel and Alabert [1989]. Indeed, each simulation has the same univariate statistics and variogram as the experimental data, and furthermore retains the measured flux value unchanged at the original measurement sites. Therefore, we cannot use a single simulation to trace degassing tectonic structures in Linosa island.

In order to show a more suitable map and define the extent of the anomalous degassing areas of Linosa island, as demonstrated by Cardellini et al. [2003], we elaborated a probability map that displays the probability that the soil CO_2 flux exceeds a threshold value at each node of the grid. Figure 6 shows a map with probability exceeding 18 g m^{-2} d^{-1}. This value was selected by inspecting the probability plot of Figure 3, and it was assumed as cutoff value separating the intermediate CO_2 flux from anomalous values. As discussed by Cardellini et al. [2003] the map in Figure 6 represents the probability that each location belongs to Diffuse Degassing Structures (DDS). These are well-defined regions of a surveyed area characterized by high levels of soil CO_2 emission and they are generally related to structural discontinuities acting as preferential pathways for gas migration towards the surface [Chiodini et al. 2001, Cardellini et al. 2003]. The map shows that in Linosa island, DDS lie manly in the eastern sector of the island and have generally a preferential NW-SE direction of elongation, corresponding to the main direction of the faults system in the Sicily Channel. The distribution of the low-energy seismic events along the axial portion of the rift system or in correspondence of the graben borders [Agius and Galea 2011], would confirm the activity of these faults. Hence, the persistent seismic activity in the SCrs would contribute to maintain a high permeability of soils driving deep fluids towards the surface.

The carbon isotopic composition of the CO_2 of three gas samples collected at 50 cm deep in the soil from two different areas showed $\delta^{13}C(CO_2)$ values versus PDB of −17.3, −14 and −8.4 ‰, respectively. Due to the low values of the soil CO_2 flux (< 80 g m^{-2} d^{-1}), the kinetic isotopic fractionation can be considered negligible in any case [Camarda et al. 2007]. The measured $\delta^{13}C$ values fall within the typical range of CO_2 with organic origin (−30 to −10 ‰ vs. PDB; Hoefs [1980], O'Learly [1988]), except for the sample with $\delta^{13}C(CO_2)$ of −8.4 ‰.

There are two possible explanations to justify the observed isotopic values. As first, the observed variability can be ascribed to different types of plants present in the island. For example, C_3 plants are characterized

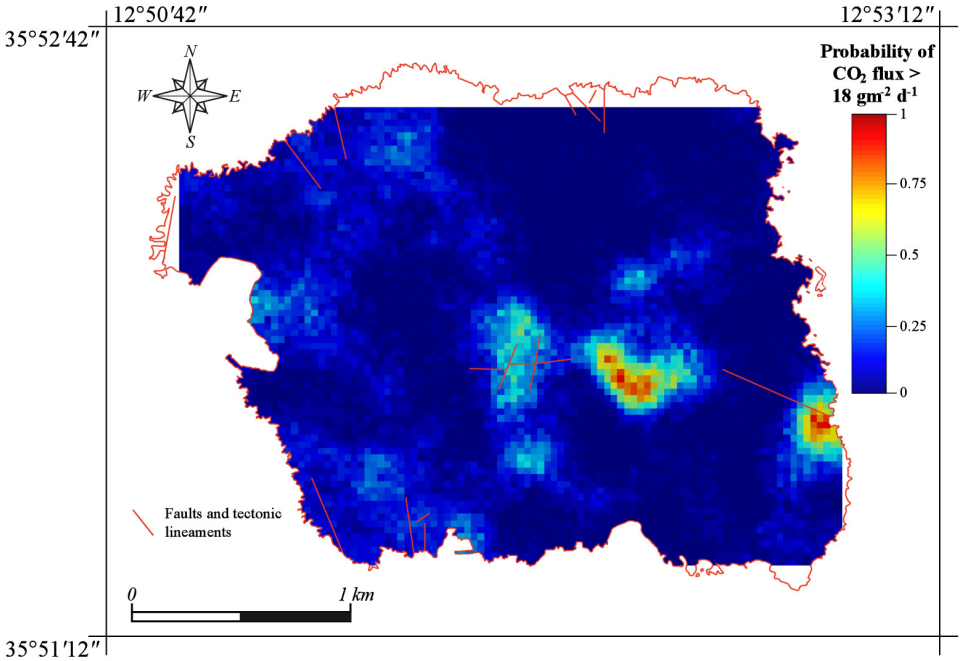

Figure 6. Map that probability exceeds the threshold value of 18 g m^{-2} d^{-1}, discriminating background from anomalous CO_2 flux. The main volcano-tectonic lineaments (red lines) by Lanzafame et al. [1994] are also reported.

by $\delta^{13}C(CO_2)$ of −27 ‰ whereas C_4 plants have value of −13 ‰ [Cheng 1996]. An alternative explanation that can explain the observed data is that the observed shift toward less negative values of $\delta^{13}C$ might be due to contribution of CO_2 from a deep (mantle) source that reaches the surface through the mapped DDS [Frezzotti et al. 2009]. However, our data do not allow us to rule out with accuracy one of these two mechanisms, and both might also coexist.

Table 2 reports the total CO_2 flux output calculated as explained above (Section 3.2). In the same table we reported for comparison the total CO_2 output estimated from other authors from some active volcanoes, tectonic and non volcanic areas in the world. As ex-

	Area (km^2)	CO_2 flux ($ton\ d^{-1}$)	CO_2 flux ($ton\ km^{-2}\ d^{-1}$)	Ref.
Cuicocha caldera, Ecuador	13.3	106 ± 5	8	Padròn et al. [2008]
Pululahua caldera, Ecuador	27.6	270 ± 19	10	Padròn et al. [2008]
Linosa	5	55 ± 0.5	11	this work
Satsuma-Iwojma volcano, Japan	2.5	80	32	Shimoike et al. [2002]
Iwojima volcano, Japan	22	760	35	Notsu et al. [2005]
Vesuvio volcano, Italy	5.5	193.8 ± 26.4	35	Frondini et al. [2004]
Mt. Epomeo, Italy	0.86	32.6 ± 2.6	38	Chiodini et al. [2004]
Nisyros caldera, Greece	2	84 ± 3.8	42	Cardellini et al. [2003]
Yanbajain geothermal field, China	3.2	138	43	Chiodini et al. [1998]
Nea Kameni island, Greece	0.28	15.4	55	Chiodini et al. [1998]
Reykjanes geothermal area, Iceland	0.22	13.5 ± 1.7	61	Fridriksson et al. [2006]
Taupo Volcanic Zone, New Zealand	8.9	620 ± 37	70	Werner and Cardellini [2006]
Vulcano (Italy)	5.4	453	84	Inguaggiato et al. [2012]
Miyakejima (summit caldera), September 1998	1.1	98	89	Hernández et al. [2001]
Ustica	4.5	712	158	Etiope et al. [1999]
Furnas caldera	5.9	959 ± 84	164	Viveiros et al. [2010]
Hakkoda region, Japan	0.58	127	219	Hernández et al. [2003]
Miyakejima (summit caldera), May 1998	0.62	146	235	Hernández et al. [2001]
Methana volcanic system, Greece	0.01	2.59	259	D'Alessandro et al. [2008]
Poggio dell'Olivo, Italy	0.82	233.5 ± 27.9	285	Cardellini et al. [2003]
Stromboli (Italy)	1.1	397	361	Inguaggiato et al. [2013]
Hot Spring Basin, Yellowstone	0.16	63 ± 20	393	Werner et al. [2008]
Mud volcano, Yellowstone	3.5	1730	494	Werner et al. [2000]
Ribeira Quente village	0.35	243 ± 43	694	Viveiros et al. [2010]
Teide volcano (summit), Spain	0.53	380	717	Hernández et al. [1998]
Liu-Huang-Ku, Taiwan	0.03	22.4	747	Lan et al. [2007]
Horseshoe Lake	0.13	104.3 ± 5	802	Cardellini et al. [2003]
Mammoth Muntain (USA), September 1997	0.145	130	897	Gerlach et al. [1998]
Albani Hills	0.06	74	1233	Chiodini and Frondini [2001]
Solfatara volcano, Italy	1	1500	1500	Chiodini et al. [2001]
Mammoth Muntain (USA), August 1995	0.145	350	2414	Gerlach et al. [1998]
Cerro Negro volcano, Nicaragua	0.58	2800	4828	Salazar et al. [2001]

Table 2. Total CO_2 flux output estimated for the island of Linosa compared with those of some active volcanoes and those of tectonic, hydrothermal or inactive volcanic areas; data are sorted based on CO_2 output in $ton\ km^{-2}\ d^{-1}$.

pected, the total CO_2 flux estimated from this study for Linosa island is low as compared with active volcanic areas, also considering the much wider areas under investigation. For instance, the flux calculated by Inguaggiato et al. [2012] in the island of Vulcano over a comparable surface, resulted to be one order of magnitude higher than the value found in Linosa. Indeed, as shown here, soil CO_2 fluxes in Linosa are only fed by superficial organic activity and degassing of mantle CO_2 through the recognized DDS. No CO_2 contribution from a hydrothermal systems, such as that identified in Vulcano island [Nuccio et al. 1999], can be claimed in case of Linosa island. Furthermore, by inspecting the CO_2 emission standardized for area (fourth column in Table 2), Linosa resulted to be one of the areas with the lowest CO_2 emission in the world. Nevertheless, his standardized value is comparable with the CO_2 emitted from the Cuicocha and Pululahua caldera in Equador [Padròn et al. 2008].

5. Conclusions

A survey of soil CO_2 diffuse degassing in Linosa island was conducted during summer 2006, over ~80% of the total surface. The island represents the oldest sub-aerial volcanic centre in the Sicily Channel (1.06 to 0.53 Ma), and to date direct evidences of related volcanic manifestations (fumaroles, thermal springs) are lacking. The results from soil CO_2 flux measurements would confirm this current state of the island. The Sequential Gaussian simulation allowed estimating total CO_2 output from the island of Linosa, which appears very low in comparison to active volcanoes and other inactive volcanic areas. In conclusion, our data showed that the actual soil CO_2 degassing in Linosa is primarily fed by CO_2 with superficial organic (biogenic) origin with a moderate contribution limited to some areas where the origin of CO_2 fluxes can be likely referred to deeper sources. By using a map of the probability that CO_2 flux would exceed a cutoff value we identified the location and the extent of the diffuse degassing structures in the eastern sector of the island. Carbon isotopic composition of CO_2 from samples collected in relatively high-flux zones would suggest a moderate contribution of CO_2 with mantle origin. However, we do not exclude the possibility of a more rigorous geochemical characterization of these gas emissions in future aimed to confirm the possibility of a degassing mantle source beneath the island of Linosa.

Acknowledgements. The project was funded by the Dipartimento della Protezione Civile (DPC-INGV Agreement 2004-2006, ProjectV5). Critical comments and helpful suggestions by the associate editor, Francesco Frondini, an anonymous reviewer and Domenico Granieri greatly improved the manuscript.

References

Agius, M.R., and P. Galea (2011). A Single-Station Automated Earthquake Location System at Wied Dalam Station, Malta, Seismol. Res. Lett., 82, 545-559.

Aiuppa, A., A. Caleca, C. Federico, S. Gurrieri and M. Valenza (2004). Diffuse degassing of carbon dioxide at Somma-Vesuvius volcanic complex (Southern Italy) and its relation with regional tectonics, J. Volcanol. Geoth. Res., 133, 55-79.

Boccaletti, M., G. Cello and L. Tortorici (1987). Transtensional tectonics in the Sicily Channel, J. Struct. Geol., 9, 869-876.

Brown, K.W., and N.J. Rosenberg (1971). Energy and CO_2 balance of an irrigated sugar beet (Beta vulgaris) field in the Great Plains, Agron. J., 63, 207-213.

Burton, M.R., G.M. Sawyer and D. Granieri (2013). Deep carbon emissions from volcanoes, Rev. Mineral. Geochem., 75 (1), 323-354.

Calanchi, N., P. Colantoni, P.L. Rossi, M. Saitta and G. Serri (1989). The Strait of Sicily continental rift system: physiography and petrochemistry of the submarine volcanic centers, Mar. Geol., 87, 55-83.

Camarda, M., S. Gurrieri and M. Valenza (2006a). In situ permeability measurements based on a radial gas advection model: Relationships between soil permeability and diffuse CO_2 degassing in volcanic areas, Pure Appl. Geophys., 163, 897-914.

Camarda, M., S. Gurrieri and M. Valenza (2006b). CO_2 flux measurements in volcanic areas using the dynamic concentration method: Influence of soil permeability, J. Geophys. Res., 111, B05202; doi:10.1029/2005JB003898.

Camarda, M., S. De Gregorio, R. Favara and S. Gurrieri (2007). Evaluation of carbon isotope fractionation of soil CO_2 under an advective–diffusive regimen: a tool for computing the isotopic composition of unfractionated deep source, Geochim. Cosmochim. Acta, 71, 3016-3027.

Camarda, M., S. De Gregorio and S. Gurrieri (2012). Magma-ascent processes during 2005-2009 at Mt. Etna inferred by soil CO_2 emissions in peripheral areas of the volcano, Chem. Geol., 330-331, 218-227; doi:10.1016/j.chemgeo.2012.08.024.

Cardellini, C., G. Chiodini and F. Frondini (2003). Application of stochastic simulation to CO_2 flux from soil: Mapping and quantification of gas release, J. Geophys. Res., 108 (B9), 2425-2437.

Cheng, W. (1996). Measurement of rhizosphere respiration and organic matter decomposition using natural ^{13}C, Plan. Soil, 183, 263-268.

Chiodini, G., R. Cioni, M. Guidi, B. Raco and L. Marini (1998). Soil CO_2 flux measurements in volcanic and geothermal areas, Appl. Geochem., 13 (5), 543-552.

Chiodini, G., and F. Frondini (2001). Carbon dioxide degassing from the Albani Hills volcanic region, Central Italy, Chem. Geol., 177 (1-2), 67-83; doi:10.1016/S0009-2541(00)00382-X.

Chiodini, G., F. Frondini, C. Cardellini, D. Granieri, L. Marini and G. Ventura (2001). CO_2 degassing and energy release at Solfatara volcano, Campi Flegrei, Italy, J. Geophys. Res., 106 (B8), 16213-16221.

Chiodini, G., R. Avino, T. Brombach, S. Caliro, C. Cardellini, S. De Vita, F. Frondini, E. Marotta and G. Ventura (2004). Fumarolic and diffuse soil degassing west of Mount Epomeo, Ischia (Italy), J. Volcanol. Geoth. Res., 133, 291-309.

Chiodini, G., S. Caliro, C. Cardellini, R. Avino, D. Granieri and A. Schmidt (2008). Isotopic composition of soil CO_2 efflux, a powerful method to discriminate different sources feeding soil CO_2 degassing in volcanic-hydrothermal areas, Earth Planet. Sci. Lett., 274, 372-379.

Ciotoli, G., M. Guerra, S. Lombardi and E. Vittori (1998). Soil gas survey for tracing seismogenic faults: a case-study in the Fucino basin (Central Italy), J. Geophys. Res., 103, 23781-23794.

Civile, D., E. Lodolo, L. Tortorici, G. Lanzafame and G. Brancolini (2010). Relationships between magmatism and tectonics in a continental rift: The Pantelleria Island region (Sicily Channel, Italy), Mar. Geol., 251, 32-46; doi:10.1016/j.margeo.2008.01.009.

D'Alessandro, W., L. Brusca, K. Kyriakopoulos, G. Michas and G. Papadakis (2008). Methana, the westernmost active volcanic system of the south Aegean arc (Greece): insight from fluids geochemistry. J. Volcanol. Geoth. Res., 178, 818-828.

De Gregorio, S., I.S. Diliberto, S. Giammanco, S. Gurrieri and M. Valenza (2002). Tectonic control over large-scale diffuse degassing in eastern Sicily (Italy), Geofluids, 2, 273-284.

Della Vedova, B., G. Pellis and E. Pinna (1989). Studio geofisico dell'area di transizione tra il Mar Pelagico e la piana abissale dello Jonio, Proc. 8th Convegno del Gruppo Nazionale di Geofisica della Terra Solida, Rome, 1, 543-558.

Diliberto, I.S., S. Gurrieri and M. Valenza (2002). Relationships between diffuse CO_2 emissions and volcanic activity on the island of Vulcano (Aeolian Islands, Italy) during the period 1984-1994, B. Volcanol., 64, 219-228.

Etiope, G., P. Beneduce, M. Calcara, P. Favali, F. Frugoni, M. Schiattarella and G. Smriglio (1999). Structural pattern and CO_2-CH_4 degassing of Ustica Island, Southern Tyrrhenian basin, J. Volcanol. Geoth. Res., 88, 291-304.

Federico, C., M. Camarda, S. De Gregorio and S. Gurrieri (2011). Long-term record of CO_2 degassing along Mt. Etna's flanks and its relationship with magma dynamics and eastern flank instability, Geochem. Geophys. Geosyst., 12; doi:10.1029/2011GC003601.

Frezzotti, M.L., A. Peccerillo and G. Panza (2009). Carbonate metasomatism and CO_2 lithosphere–asthenosphere degassing beneath the western Mediterranean: an integrated model arising from petrological and geophysical data, Chem. Geol., 262, 108-120; doi:10.1016/j.chemgeo.2009.02.015.

Fridriksson, T., B.R. Kristjánsson, H. Ármannsson, E. Margrétardóttir, S. Ólafsdóttir and G. Chiodini (2006). CO_2 emissions and heat flow through soil, fumaroles, and steam heated mud pools at the Reykjanes geothermal area, SW Iceland, Appl. Geochem., 21, 1551-1569.

Frondini, F., G. Chiodini, S. Caliro, C. Cardellini, D. Granieri and G. Ventura (2004). Diffuse CO_2 degassing at Vesuvio, Italy, B. Volcanol., 66, 642-651.

Gemmellaro, C. (1831). Relazione dei fenomeni del nuovo vulcano sorto dal mare fra la costa di Sicilia e l'isola di Pantelleria nel mese di luglio 1831, Atti Accad. Gioenia Catania, 8, 271-298.

Gerlach, T.M., M.P. Doukas, K.A. McGee and R. Kessler (1998). Three-year decline of magmatic CO_2 emissions from soils of a Mammoth Mountain tree kill: Horseshoe Lake, CA, 1995-1997, Geophys. Res. Lett., 25, 1947-1950.

Giammanco, S., S. Gurrieri and M. Valenza (1995). Soil CO_2 degassing on Mt. Etna (Sicily) during the period 1989-1993: discrimination between climatic and volcanic influences, B. Volcanol., 57, 52-60.

Giammanco, S., S. Gurrieri and M. Valenza (1997). Soil CO_2 degassing along tectonic structures of Mt. Etna Sicily: the Pernicana Fault, Appl. Geochem., 12, 429-436.

Giammanco, S., S. Gurrieri and M. Valenza (2006). Fault-controlled soil CO_2 degassing and shallow magma bodies: summit and lower East Rift of Kilauea volcano (Hawaii), 1997, Pure Appl. Geophys., 163, 853-867.

Granieri, D., G. Chiodini, W. Marzocchi and R. Avino (2003). Continuous monitoring of CO_2 soil diffuse degassing at Phlegraean Fields (Italy): Influence of environmental and volcanic parameters, Earth Planet. Sci. Lett., 212, 167-179.

Grasso, M., G. Lanzafame, P.L. Rossi, H.U. Schmincke, A.C. Tranne, J. Lajoie and E. Lanti (1991). Volcanic evolution of the island of Linosa. Strait of Sicily, Mem. Soc. Geol. It., 47, 509-525.

Guerra, M., and S. Lombardi (2001). Soil-gas method for tracing neotectonic faults in clay basins: the Pisticci field (Southern Italy), Tectonophysics, 339,

511-522.

Gurrieri, S., and M. Valenza (1988). Gas transport in natural porous mediums: a method for measuring CO_2 flows from the ground in volcanic and geothermal areas, Rend. Soc. It. Min. Petrogr., 43, 1151-1158.

Harris, D.M., and W.I. Rose (1996). Dynamics of carbon dioxide emissions, crystallization, and magma ascent: hypotheses, theory, and applications to volcano monitoring at Mount St. Helens, B. Volcanol., 58, 163-174.

Hernández, P.A., N.M. Pérez, J.M. Salazar, S. Nakai, K. Notsu and H. Wakita (1998). Diffuse emission of carbon dioxide, methane, and helium-3 from Teide Volcano, Tenerife, Canary Islands, Geophys. Res. Lett., 25 (17), 3311-3314.

Hernández, P.A., J.M. Salazar, Y. Shimoike, T. Mori, K. Notsu and N. Pérez (2001). Diffuse emission of CO_2 from Miyakejima volcano, Japan. Chem. Geol., 177, 175-185.

Hernández, P., K. Notsu, M. Tsurumi, T. Mori, M. Ohno, Y. Shimoike, J. Salazar and N. Pérez (2003). Carbon dioxide emissions from soils at Hakkoda, north Japan, J. Geophys. Res., 108 (B4), 2210; doi:10.1029/2002JB001847.

Hoefs, J. (1980). Stable Isotope Geochemistry, Springer-Verlag, Berlin, 280 pp.

Inguaggiato, S., A. Mazot, I.S. Diliberto, C. Inguaggiato, P. Madonia, D. Rouwet and F. Vita (2012). Total CO_2 output from Vulcano island (Aeolian Islands, Italy), Geochem. Geophys. Geosyst., 13; doi:10.1029/2011GC003920.

Inguaggiato, S., M.P. Jácome Paz, A. Mazot, H. Delgado Granados, C. Inguaggiato and F. Vita (2013). CO_2 output discharged from Stromboli Island (Italy), Chem. Geol., 339, 52-60.

Journel, A.G., and F. Alabert (1989). Non-Gaussian data expansion in the Earth sciences, Terra Nova, 1 (2), 123-134.

Klinkenberg, L.J. (1941). The permeability of porous media to liquids and gases, Drill. Prod. Prac., API, New York, 200-213.

Lan, T.F., T.F. Yang, H.-F. Lee, Y.-G. Chen, C.-H. Chen, S.-R. Song and S. Tsao (2007). Compositions and flux of soil gas in Liu-Huang-Ku hydrothermal area, northern Taiwan, J. Volcanol. Geoth. Res., 165, 32-45.

Lanti, E.G., Lanzafame, P.L. Rossi, C.A. Tranne and N. Calanchi (1988). Vulcanismo e tettonica nel Canale di Sicilia: l'isola di Linosa, Miner. Petrogr. Acta, 31, 69-93.

Lanzafame, G., P.L. Rossi, C.A. Tranne and E. Lanti (1994). Carta geologica di Linosa, 1:5000, S.EL.CA., Firenze.

Lewicki, J.L., and S.L. Brantley (2000). CO_2 degassing along the San Andreas fault, Parkfield, California, Geophys. Res. Lett., 27 (1), 5-8.

Lodolo, E., D. Civile, C. Zanolla and R. Geletti (2012). Magnetic signature of the Sicily Channel volcanism, Mar. Geophys. Res., 33, 33-44.

Moldrup, P., S. Yoshikawa, T. Olesen, T. Komatsu and D.E. Rolston (2003). Gas diffusivity in undisturbed volcanic ash soils: Test of soil-water-characteristic-based prediction models, Soil Sci. Soc. Am. J., 67, 41-51.

Monteith, J.L., G. Szeicz and K. Yabuki (1964). Crop photosynthesis and the flux of carbon dioxide below the canopy, J. Appl. Ecol., 1, 321-327.

Notsu, K., K. Sugiyama, M. Hosoe, A. Uemura, Y. Shimoike, F. Tsunomori, H. Sumino, J. Yamamoto, T. Mori and P.A. Hernández (2005). Diffuse CO_2 efflux from Iwojima volcano, Izu-Ogasawara arc, Japan, J. Volcanol. Geoth. Res., 139, 147-161.

Nuccio, P.M., A. Paonita and F. Sortino (1999). Geochemical modeling of mixing between magmatic and hydrothermal gases: the case of Vulcano Island, Italy, Earth Planet. Sci. Lett., 167, 321-333.

O'Leary, M.H. (1988). Carbon isotopes in photosynthesis, Bioscience, 38, 328-336.

Padrón, E., P.A. Hernandéz, T. Toulkeridis, N.M. Pérez, R. Marrero, G. Melián, G. Virgili and K. Notsu (2008). Diffuse CO_2 emission rate from Pululahua and the lake-filled Cuicocha calderas, Ecuador, J. Volcanol. Geoth. Res., 176, 163-169.

Remy, N. (2005). S-GEMS: the Stanford Geostatistical Modeling Software: a tool for new algorithms development, In: O. Leuangthong and C. Deutsch (eds.), Geostatistics Banff 2004: 7th International Geostatistics Conference, Quantitative Geology and Geostatistics, Springer, Banff, 865-871.

Rinaldi, A.P., J. Vandemeulebrouck, M. Todesco and F. Viveiros (2012). Effects of atmospheric conditions on surface diffuse degassing, J. Geophys. Res., 117, B11201; doi:10.1029/2012JB009490.

Rotolo, S.G., F. Castorina, D. Cellura and M. Pompilio (2006). Petrology and Geochemistry of Submarine Volcanism in the Sicily Channel Rift, J. Geol., 114, 355-365.

Salazar, J.M.L., P.A. Hernández, N.M. Pérez, G. Melián, J. Álvarez, F. Segura and K. Notsu (2001). Diffuse emission of carbon dioxide from Cerro Negro Volcano, Nicaragua, Central America, Geophys. Res. Lett., 28 (22), 4275-4278.

Scarascia, S., R. Cassinis, A. Lozej and A. Nebuloni (2000). A seismic and gravimetric model of crustal structures across the Sicily Channel Rift Zone, B. Soc. Geol. Ital. 119, 213-222.

Schorlemmer, D., F. Mele and W. Marzocchi (2010). A

completeness analysis of the National Seismic Network of Italy, J. Geophys. Res., 115, B04308; doi:10.1029/2008JB006097.

Shimoike, Y., K. Kazahaya and H. Shinohara (2002). Soil gas emission of volcanic CO_2 at Satsuma-Iwojima volcano, Japan, Earth Planets Space, 54, 239-247.

Sinclair, A.J. (1974). Selection of threshold values in geochemical data using probability graphs, J. Geochem. Explor., 3, 129-149.

Viveiros, F., C. Cardellini, T. Ferreira, S. Caliro, G. Chiodini and C. Silva (2010). Soil CO_2 emissions at Furnas volcano, São Miguel Island, Azores archipelago: Volcano monitoring perspectives, geomorphologic studies, and land use planning application, J. Geophys. Res., 115, B12208; doi:10.1029/2010JB007555.

Washington, H.S. (1909). The submarine eruption of 1831 and 1891 near Pantelleria, Am. J. Sci., 27, 131-150.

Werner, C., S.L. Brantley and K. Boomer (2000). CO_2 emissions related to the Yellowstone volcanic system. Statistical sampling, total degassing, and transport mechanisms, J. Geophys. Res., 105 (B5), 10831-10846.

Werner, C., and C. Cardellini (2006). Comparison of carbon dioxide emissions with fluid upflow, chemistry, and geologic structures at the Rotorua geothermal system, New Zealand, Geothermics, 35, 221-238.

Werner, C., S. Hurwitz, W.C. Evans, J.B. Lowenstern, D. Bergfeld, H. Heasler, C. Jaworowski and A. Hunt (2008). Volatile emissions and gas geochemistry of Hot Spring Basin, Yellowstone National Park, USA, J. Volcanol. Geoth. Res., 178, 751-762.

*Corresponding author: Marco Camarda,
Istituto Nazionale di Geofisica e Vulcanologia, Sezione di Palermo, Palermo, Italy; e-mail: marco.camarda@ingv.it.